Electronic Supplementary Material (ESI) for Nanoscale.

Supporting Information

Turbostratic-Carbon-Localised FeS_2 Nanocrystals as Anode for High Performance Sodium-Ion Batteries

Yanyan Liu[a], Long Zhang[a,*], Di Liu[a], Wentao Hu[a], XinlinYan[b], ChuangYu[c], Hong Zeng[d], TongdeShen[a]

[a]Clean Nano Energy Center, State Key Laboratory of Metastable Materials Science and Technology, Yanshan University, Qinhuangdao, Hebei 066004, China

[b]Institute of Solid State Physics, Vienna University of Technology, WiednerHauptstr. 8-10, 1040 Vienna, Austria

[c]Department of Mechanical and Materials Engineering, University of Western Ontario, 1151 Richmond St, London, Ontario, N6A 3K7, Canada

[d]Beijing Key Laboratory of Energy Nanomaterials, Advance Technology & Materials Co., Ltd, China Iron & Steel Research Institute Group, Beijing 100081, PR China

*Corresponding author. E-mail address: lzhang@ysu.edu.cn (Long Zhang)

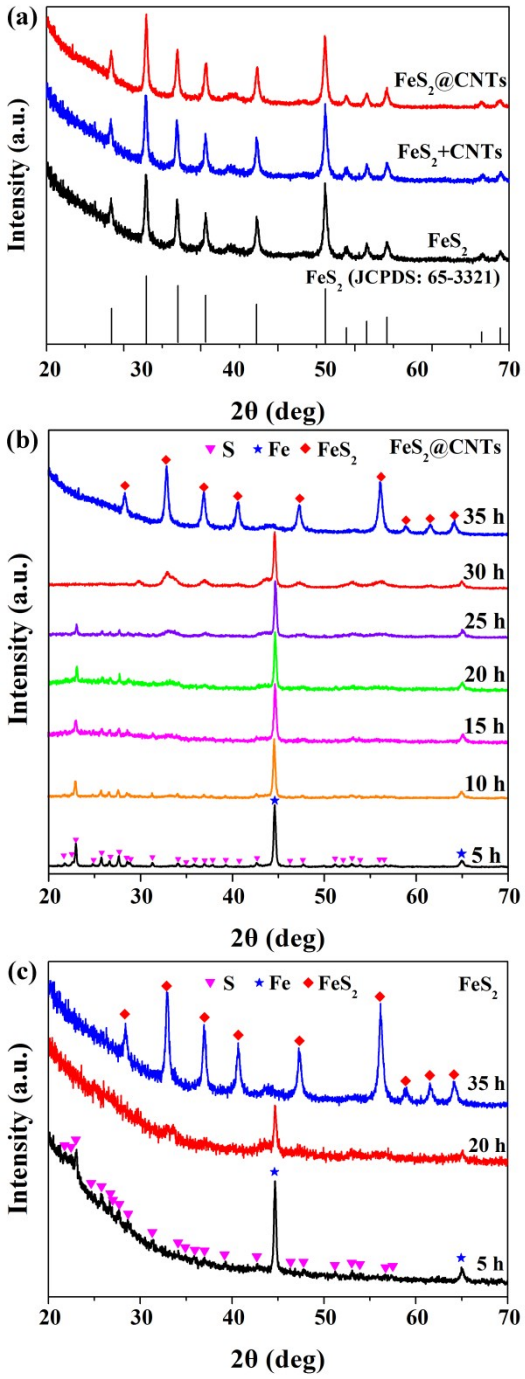

Figure S1. (a) XRD patterns of FeS_2@CNTs and FeS_2 after mechanical milling for 35 h and FeS_2+CNTs ball milling for 5 h. The Bragg positions of the pyrite FeS_2 with Pa-3 symmetry are indexed accordingly. XRD patterns of FeS_2@CNTs (b) and FeS_2 (c) for various mechanical alloying times.

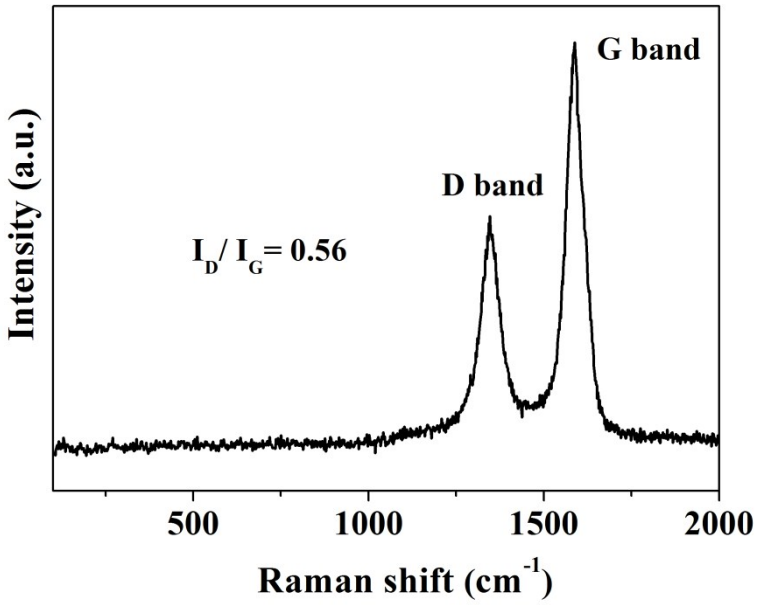

Figure S2. Raman spectrum of the pristine CNTs.

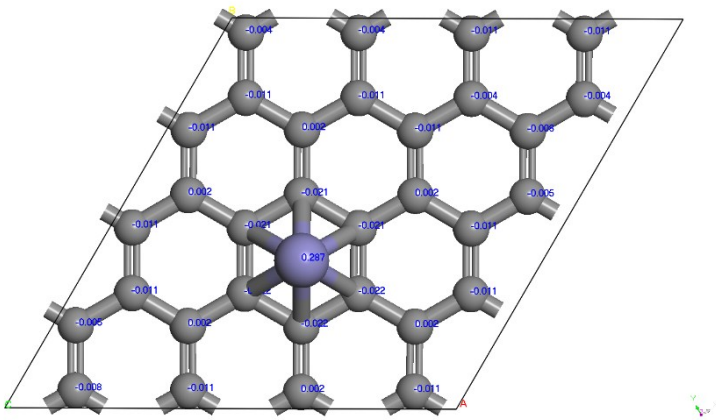

Figure S3. Charge transfer between Fe and C atoms.

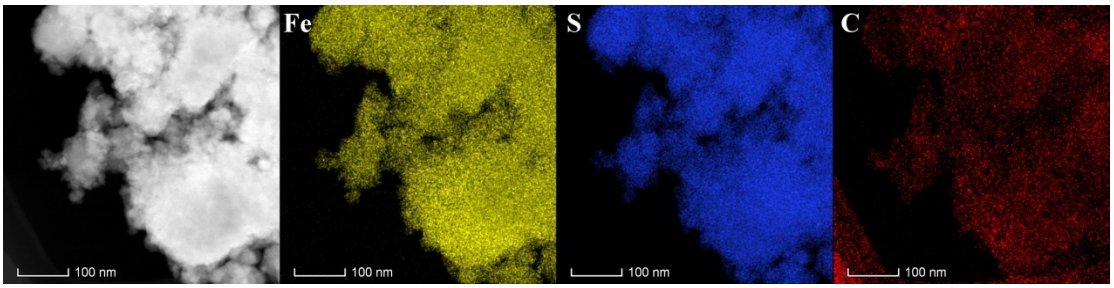

Figure S4. Elemental mapping of the as-prepared FeS_2@CNTs.

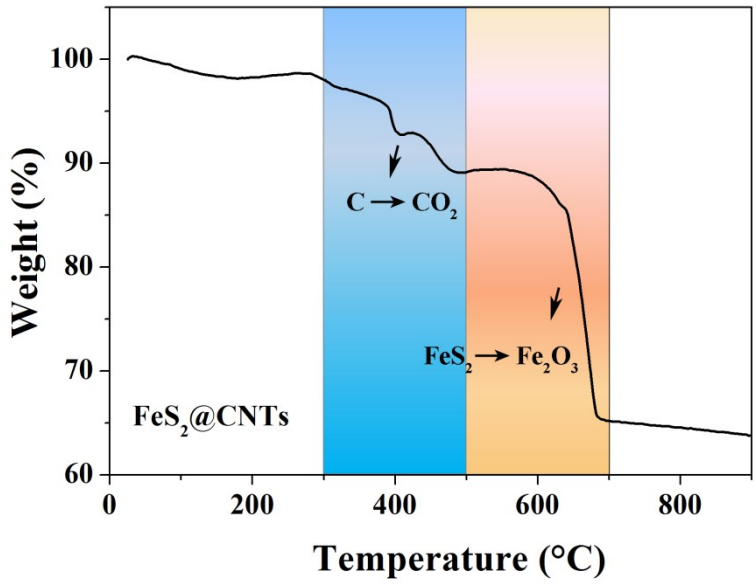

Figure S5. TGA curve of FeS_2@CNTs under air atmosphere.

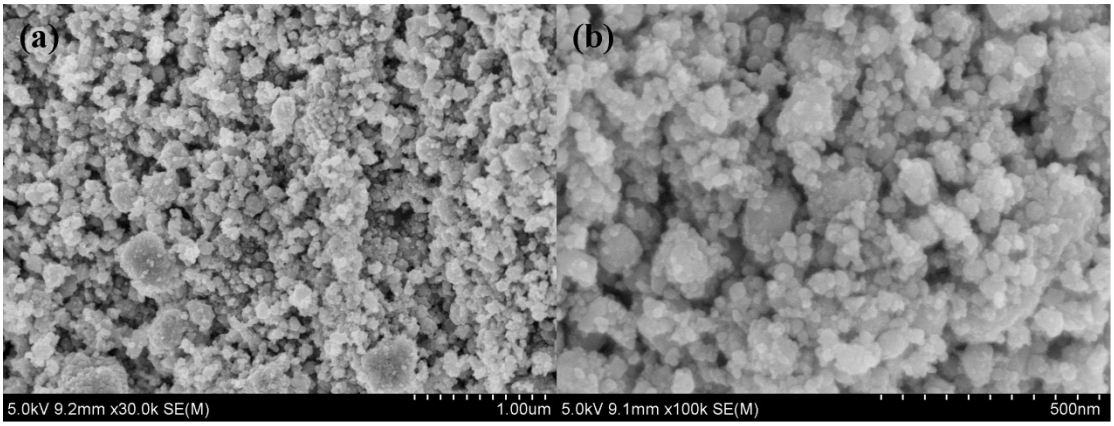

Figure S6. SEM images of FeS_2 under low (a) and high magnifications (b).

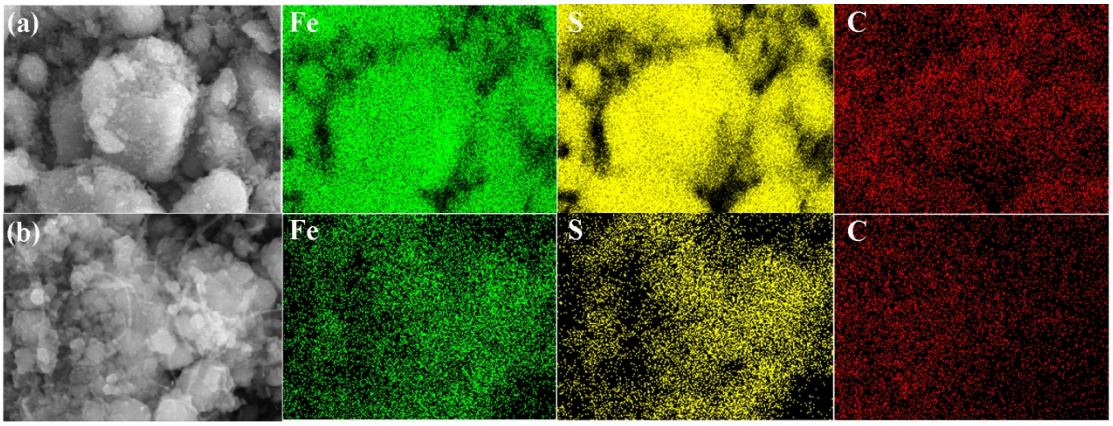

Figure S7. Element mapping of FeS_2@CNTs (a) and FeS_2+CNTs (b).

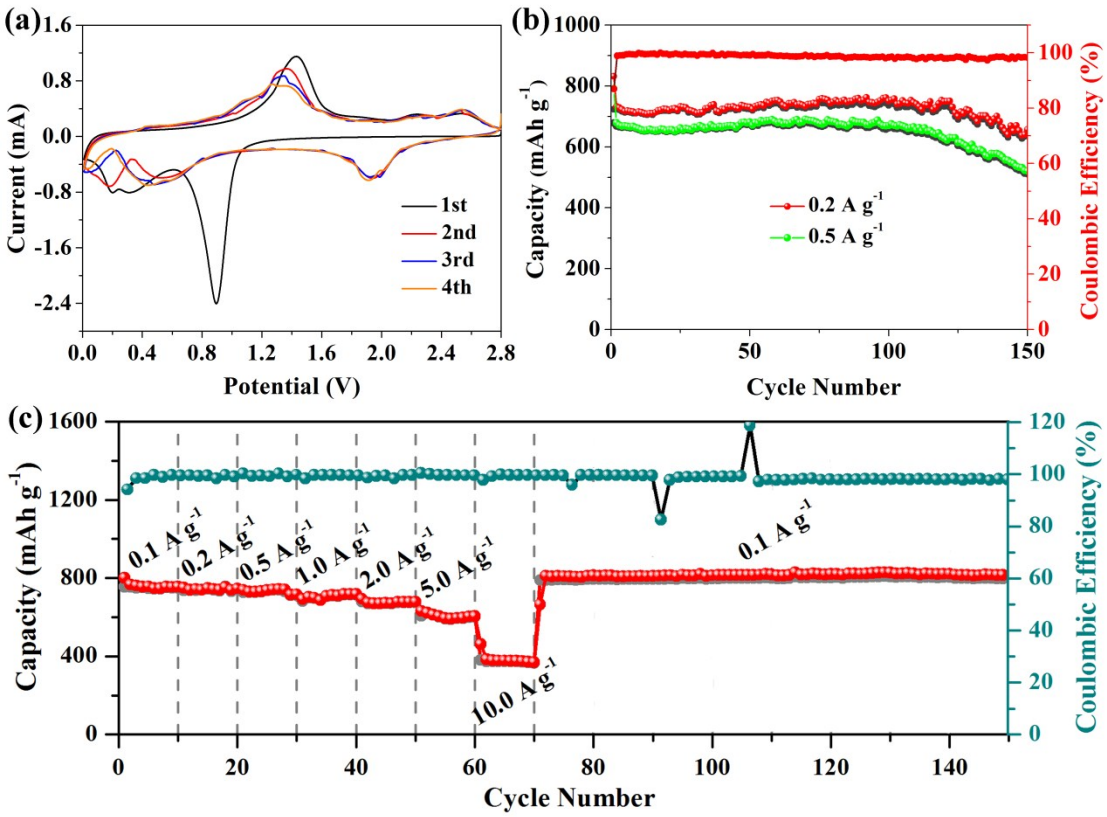

Figure S8. The electrochemical performance of FeS_2@CNTs at a cut off voltage of 0.01−2.8 V. (a) CV curves for the first four cycles at a scan rate of 0.2 mV s^{-1}. (b) Cycling performance at currenties density of 0.2 A g^{-1} and 0.5 A g^{-1}. (c) Rate performance at various current densities.

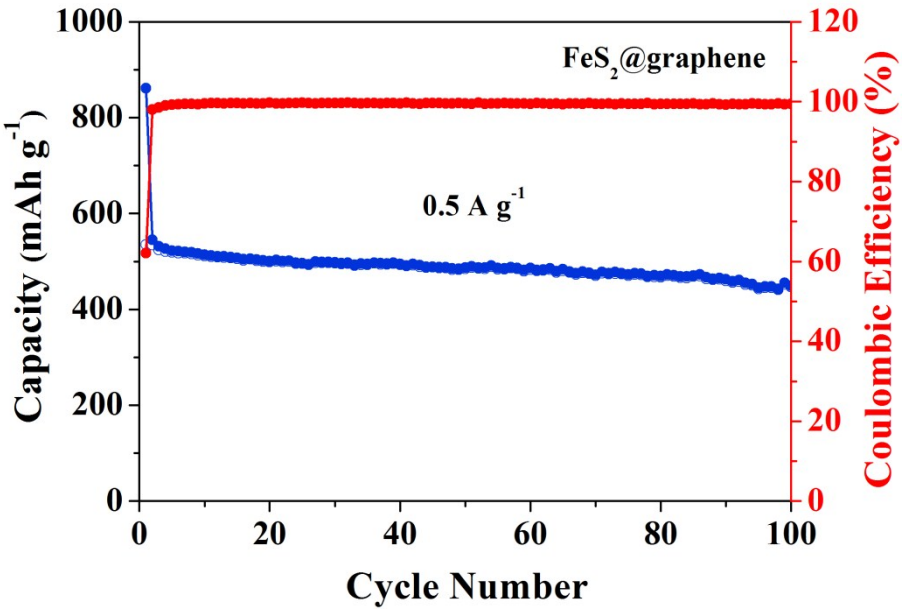

Figure S9. Cycling performance and coulombic efficiency of a FeS_2@graphene composite at a current density of 0.5 A g^{-1}.

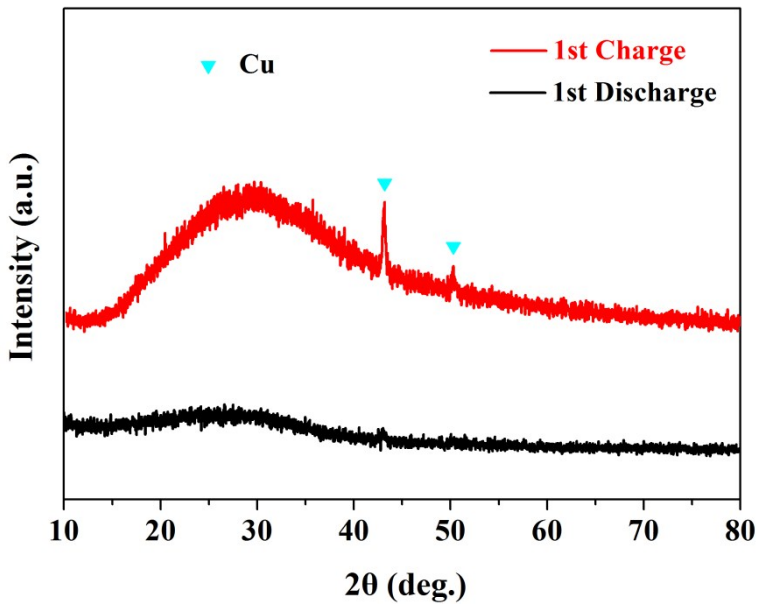

Figure S10. *Ex situ* XRD patterns of FeS_2@CNTs after fully discharging and charging.

Table S1. Elemental Analysis of FeS_2@CNTs.

	Atomic ratio (%)			atomic ratio normalized to Fe			wt%		
	Fe	S	C	Fe	S	C	Fe	S	C
FeS_2@CNTs	28.30	57.75	13.95	1	2.04	0.49	44.02	51.33	4.65

Table S2 Comparation of the electrochemical properties of iron sulfides anodes for NIBs

Anode	Fe/S loading (%)	Cut-off voltage (V)	Current density (A g^{-1})	Specific capacity (mAh g^{-1})	Note
FeS_2@C	85.5	0.01-2	0.1	511	Ref.50
FeS_2@C-2h	48.5	0.1-2	0.1	543	Ref.52
$Fe_{1-x}S$@CNTs	70.4	0.01-2.3	0.2	493	Ref.42
$Fe_{1-x}S$@NC@G	62.5	0.01-2.5	0.2	400	Ref.19
FeS_2@NSC/G	48	0.01-2.5	0.1	420	Ref.54
$Fe_{1-x}S$@NC	66.4	0.01-2.5	0.1	594	Ref.30
rGO@p-FeS_2@C	81.1	0.01-2.8	0.1	619	Ref.58
G@Y-S FeS_2@C	40	0.01-2.8	0.2	521	Ref.59
FeS_2@G@CNF	94	0.01-3	0.1	406	Ref.45
Fe_7S_8@C NCs	89.48	0.01-3	0.09	700	Ref.12
FeS_2@C	83.2	0.01-3	0.1	620	Ref.60
CL-C/FeS	76.45	0.01-3	0.1	466	Ref.61
Fe_7S_8 NPs	74.74	0.01-3	0.1	705	Ref.15
FeS_2@CNTs	95.24	0.01-2 0.01-2.8	0.1 0.1	542 755	This work